

AD-A257 878



2

# NAVAL POSTGRADUATE SCHOOL Monterey, California



DTIC  
ELECTE  
DEC 08 1992  
S B D

## THESIS

STABILITY OF TURNING RATE GUIDANCE  
AND CONTROL LAWS FOR AUTONOMOUS VEHICLES

by

Ioannis Kapelios

June, 1992

Advisor:

Fotis A. Papoulias

Approved for public release; distribution is unlimited.

92-31054



UNCLASSIFIED

SECURITY CLASSIFICATION OF THIS PAGE

## REPORT DOCUMENTATION PAGE

1a. REPORT SECURITY CLASSIFICATION Unclassified			1b. RESTRICTIVE MARKINGS		
2a. SECURITY CLASSIFICATION AUTHORITY			3. DISTRIBUTION/AVAILABILITY OF REPORT Approved for public release; distribution is unlimited.		
2b. DECLASSIFICATION/DOWNGRADING SCHEDULE					
4. PERFORMING ORGANIZATION REPORT NUMBER(S)			5. MONITORING ORGANIZATION REPORT NUMBER(S)		
6a. NAME OF PERFORMING ORGANIZATION Naval Postgraduate School		6b. OFFICE SYMBOL (If applicable) 33		7a. NAME OF MONITORING ORGANIZATION Naval Postgraduate School	
6c. ADDRESS (City, State, and ZIP Code) Monterey, CA 93943-5000			7b. ADDRESS (City, State, and ZIP Code) Monterey, CA 93943-5000		
8a. NAME OF FUNDING/SPONSORING ORGANIZATION		8b. OFFICE SYMBOL (If applicable)		9. PROCUREMENT INSTRUMENT IDENTIFICATION NUMBER	
8c. ADDRESS (City, State, and ZIP Code)			10. SOURCE OF FUNDING NUMBERS		
			Program Element No.	Project No.	Task No.
					Work Unit Accession Number
11. TITLE (Include Security Classification) STABILITY OF TURNING RATE GUIDANCE AND CONTROL LAW FOR AUTONOMOUS VEHICLES					
12. PERSONAL AUTHOR(S) Kapelios, Ioannis					
13a. TYPE OF REPORT Master's Thesis		13b. TIME COVERED From To		14. DATE OF REPORT (year, month, day) June 1992	
				15. PAGE COUNT 49	
16. SUPPLEMENTARY NOTATION The views expressed in this thesis are those of the author and do not reflect the official policy or position of the Department of Defense or the U.S. Government.					
17. COSATI CODES			18. SUBJECT TERMS (continue on reverse if necessary and identify by block number)		
FIELD	GROUP	SUBGROUP	Stability, guidance, control, autonomous vehicles		
19. ABSTRACT (continue on reverse if necessary and identify by block number) The problem of turning rate guidance and control for autonomous vehicles is analyzed. Control design is based on the dynamic equations of motion for lateral motions, sway and yaw, while guidance design is based on the kinematics. Analytical conditions are derived that enable the two schemes to operate simultaneously without loss of stability. The results are verified by direct numerical integrations of the equations of motion.					
20. DISTRIBUTION/AVAILABILITY OF ABSTRACT <input checked="" type="checkbox"/> UNCLASSIFIED/UNLIMITED <input type="checkbox"/> SAME AS REPORT <input type="checkbox"/> DTIC USERS			21. ABSTRACT SECURITY CLASSIFICATION Unclassified		
22a. NAME OF RESPONSIBLE INDIVIDUAL F. A. Papoulas			22b. TELEPHONE (Include Area code) (408) 646-3381		22c. OFFICE SYMBOL 31

DD FORM 1473, 84 MAR

83 APR edition may be used until exhausted  
All other editions are obsoleteSECURITY CLASSIFICATION OF THIS PAGE  
UNCLASSIFIED

Approved for public release; distribution is unlimited.

Stability of Turning Rate Guidance and  
Control Laws for Autonomous Vehicles

by

Ioannis Kapelios  
Lieutenant Colonel, Hellenic Army  
B.S., Hellenic Army Academy, 1972

Submitted in partial fulfillment  
of the requirements for the degree of

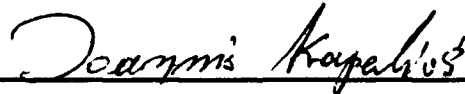
MASTER OF SCIENCE IN ENGINEERING SCIENCE

from the

NAVAL POSTGRADUATE SCHOOL

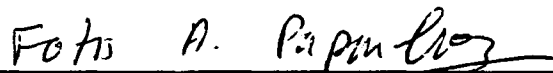
June 1992

Author:



Ioannis Kapelios

Approved by:



Fotis A. Papoulas, Thesis Advisor



Louis V. Schmidt, Second Reader



Daniel J. Collins, Chairman  
Department of Aeronautics

# ABSTRACT

The problem of turning rate guidance and control for autonomous vehicles is analyzed. Control design is based on the dynamic equations of motion for lateral motions, sway and yaw, while guidance design is based on the kinematics. Analytical conditions are derived that enable the two schemes to operate simultaneously without loss of stability. The results are verified by direct numerical integrations of the equations of motion.

DTIC QUALITY INSPECTED 2

Accession For	
NTIS GRA&I	<input checked="" type="checkbox"/>
DTIC TAB	<input type="checkbox"/>
Unannounced	<input type="checkbox"/>
Justification	
By	
Distribution/	
Availability Codes	
Dist	Avail and/or Special
A-1	

## TABLE OF CONTENTS

I.	INTRODUCTION . . . . .	1
II.	EQUATIONS OF MOTION . . . . .	3
III.	CONTROL LAW DESIGN . . . . .	7
	A. LINEARIZATION . . . . .	7
	B. FEEDBACK CONTROL . . . . .	8
	C. FEEDFORWARD CONTROL . . . . .	10
	D. RESULTS . . . . .	11
	E. ACCURACY . . . . .	12
	F. INTEGRAL CONTROL . . . . .	18
IV.	GUIDANCE LAW . . . . .	22
	A. GENERAL . . . . .	22
	B. CROSS TRACK ERROR GUIDANCE . . . . .	22
	C. PROPORTIONAL GUIDANCE . . . . .	25
V.	STABILITY . . . . .	27
	A. SIMULATIONS . . . . .	27

B. STABILITY . . . . .	28
------------------------	----

VI. CONCLUSIONS AND RECOMMENDATIONS . . . . .	37
---	----

List of References . . . . .	38
------------------------------	----

Initial Distribution list . . . . .	39
-------------------------------------	----

## LIST OF FIGURES

Figure 1. Vehicle Geometry and Definitions of Symbols.	6
Figure 2. Turning Rate Response for $T_c=1$ .	13
Figure 3. Turning Rate Response for Different Values of $T_c$ .	14
Figure 4. Rudder Angle Time Histories for Different Values of $T_c$ .	15
Figure 5. Turning Rate Response for Different Values of $T_c$ and for Nonzero Drag Coefficient.	17
Figure 6. Turning Rate Response for $T_c=1$ , Different values of $T_i$ , Nonzero Drag Coefficient, and Use of Integral Control.	21
Figure 7. Path Keeping Response for $T_c=0.5$ , $T_c=1$ .	32
Figure 8. Path Keeping Response for $T_c=0.5$ , $T_c=0.5$ .	33
Figure 9. Path Keeping Response for $T_c=2$ , $T_c=0.5$ .	34
Figure 10. Path Keeping Response for $T_c=2$ , $T_c=2$ .	35
Figure 11. Critical $T_c$ , $T_c$ Curve for Stability.	36

#### ACKNOWLEDGEMENTS

The author wishes to thank Dr. Fotis Papoulias for his help in this work, and Dr. Louis V. Schmidt for his assistance during his studies at the Naval Postgraduate school. The completion of this work owes much to the love and support of my wife Kalliopi and my three children Christos, Melina and Panayiotis. Finally, the author would like to thank the Hellenic Army for the opportunity it gave him to pursue higher education.



## I. INTRODUCTION

Autonomous vehicles that are suitable for use in both naval and commercial operations, have unique mission requirements and dynamic characteristics. In particular, they are required to be highly maneuverable and very responsive as they operate in obstacle avoidance and object recognition tasks. The need therefore, arises to maintain accurate path keeping in confined spaces under the influence of steady and time varying external excitation. The primary vehicle guidance system is based on heading or turning rate commands that are generated based on a specified geographical sequence of desired way points. These guidance commands are then passed to the vehicle controller which attempts to deliver the commanded heading and/or heading rate of change by an appropriate use of the vehicle control surfaces [Ref.1]. For vehicle operations in confined spaces the way point sequence must be very dense so that satisfactory path accuracy is maintained.

One efficient way of maneuvering through a given way point sequence is by using a line of sight guidance law which commands a heading angle that is directly related to the line of sight angle between the vehicle position and a desired destination point. The vehicle controller is then an orientation control law which delivers the commanded heading.

Previous studies [Ref.2], have demonstrated that this scheme is guaranteed stable only if the way point separation is above some critical value. This conclusion is true regardless of the particular form of the line of sight guidance or the heading control law used. In this work we analyze the turning rate guidance and control problem where the guidance law demands a specific yaw rate response from the controller. A linear state feedback with a feedforward term [Ref.3], control law is used, while two different guidance schemes are considered. The first is a cross track error guidance law which is very popular in land based robotic applications [Ref.4]. The second is a proportional guidance law which is based on the line of sight angle between the vehicle and a target point. Stability analysis is performed and numerical integrations are used to confirm the theoretical results. All numerical computations in this work are performed for the Naval Postgraduate School autonomous vehicle, for which a complete set of geometric properties and hydrodynamic characteristics is available [Ref.5].

## II. EQUATIONS OF MOTION

Restricting our attention to the horizontal plane, the mathematical model consists of the nonlinear sway (translational motion parallel to the vehicle longitudinal axis) and yaw (rotational motion about the vertical axis) equations of motion. In a moving coordinate frame fixed at the vehicle's geometrical center (see Fig.1), Newton's equations of motion are:

$$m(\dot{v} + ur + x_G \dot{r}) = Y \quad (1)$$

$$I_z \dot{r} + mx_G(\dot{v} + ur) = N, \quad (2)$$

where  $m$  is the mass of the vehicle,  $I_z$  its moment of inertia with respect to the vertical axis,  $u$  the forward velocity,  $x_G$  the coordinate of the vehicle center of gravity with respect to its centroid,  $v$  and  $r$  are the relative sway and yaw velocities of the moving vehicle with respect to the water; and  $Y$ ,  $N$  represent the total excitation sway force and yaw moment, respectively.

Following standard vehicle maneuvering assumptions, these forces can be expressed as the sum of quadratic drag terms and first order polynomials in  $v$  and  $r$  with constant coefficients. In this way the nonlinear equations of motion in the horizontal plane become

$$m(\dot{v}+ur+x_G\dot{r})=Y_r\dot{r}+Y_v\dot{v}+Y_rur+Y_vuv+Y_\delta u^2\delta-\int C_D h(\xi)(v+\xi r)|v+\xi r|d\xi \quad (3)$$

$$I_z\dot{r}+mx_G(\dot{v}+ur)=N_r\dot{r}+N_v\dot{v}+N_rur+N_vuv+N_\delta u^2\delta-0.5\rho\int C_D h(\xi)(v+\xi r)|v+\xi r|\xi d\xi \quad (4)$$

In equation 3 the terms  $Y_{\dot{r}}$ ,  $Y_{\dot{v}}$  represent the change in the lateral force due to unit changes in the angular acceleration  $\dot{r}$  and the lateral translational acceleration  $\dot{v}$ , respectively. Likewise, the terms  $Y_v$ ,  $Y_r$  represent the change in the lateral force due to unit changes in the corresponding velocities  $v$  and  $r$ . The terms  $N_{\dot{r}}$ ,  $N_{\dot{v}}$ ,  $N_r$ ,  $N_v$  in equation 4 are defined similarly.  $C_D$  is the drag coefficient and  $\delta$  is the rudder angle. The NPS AUV II is equipped with both stern and bow rudder which are identical in size and are deflected in opposite directions for maximum maneuverability. In other words

$$\delta_s=\delta, \quad \delta_b=-\delta \quad (5)$$

where  $\delta_s$  is the stern rudder angle, and  $\delta_b$  the bow rudder angle. The cross flow integral drag terms in the equations of motion become important for hovering operations or low speed maneuvering, whereas at high speeds  $u$  the steering response is predominantly linear.

To complete the model, we need the expressions for the vehicle yaw rate

$$\dot{\Psi} = r, \quad (6)$$

and the inertial position rates

$$\dot{x} = u \cos \Psi - v \sin \Psi, \quad (7)$$

$$\dot{y} = u \sin \Psi + v \cos \Psi, \quad (8)$$

where  $\delta_0$  is the vehicle heading angle as shown in Figure 1. Although it is recognized that the steering gear is both rate and angle limited, steering gear dynamics are not included in the formulation since they are much faster than the dynamics of a turning vehicle. The methods presented in the following sections can easily accommodate such modifications if desired.

The surge velocity  $u$  is clearly affected during the trim due to the added drag in turning. For the purposes of this study, it is assumed to be constant. This is a valid approximation since experimental experience has shown that the propulsion control law is in general capable of keeping the forward speed  $u$  relatively constant at the commanded value.

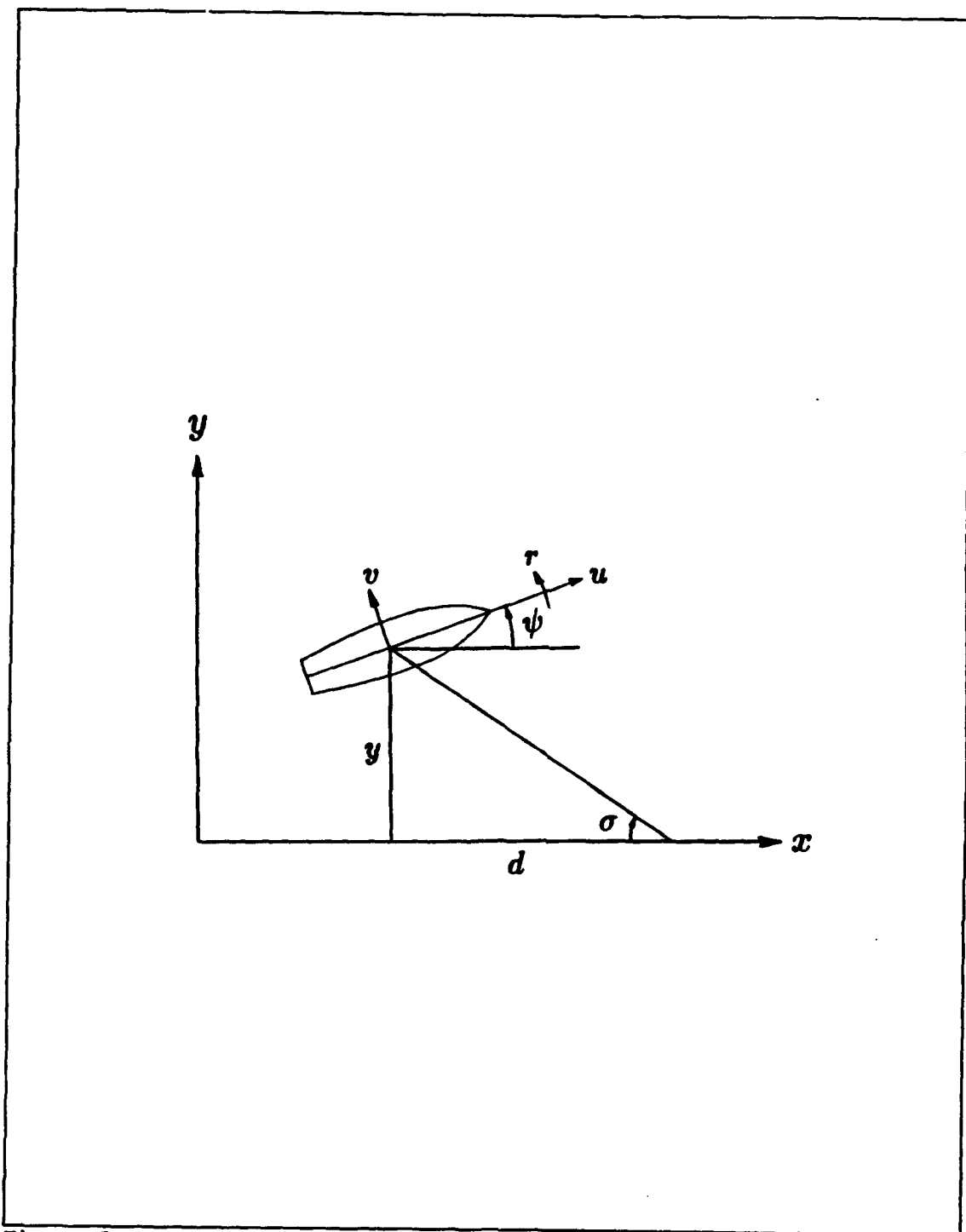


Figure 1. Vehicle Geometry and Definitions of Symbols.

### III. CONTROL LAW DESIGN

#### A. LINEARIZATION

As was mentioned in the previous chapter, during regular cruising operations at about 2 ft/sec forward speed, the nonlinear term in the equations of motion 3 and 4 are small and, therefore, effective control can be maintained by using their linear form

$$m(\dot{v} + u r + x_G \dot{r}) = Y_t \dot{r} + Y_v \dot{v} + Y_r u r + Y_v u v + Y_\delta u^2 \delta. \quad (9)$$

$$I_z \dot{r} + m x_G (\dot{v} + u r) = N_t \dot{r} + N_v \dot{v} + N_r u r + N_v u v + N_\delta u^2 \delta. \quad (10)$$

After some algebra, equations 9 and 10 can be put into state space form as

$$\dot{v} = a_{11} u v + a_{12} u r + b_1 u^2 \delta, \quad (11)$$

$$\dot{r} = a_{21} u v + a_{22} u r + b_2 u^2 \delta, \quad (12)$$

where

$$D a_{11} = (I_z - N_t) Y_v - (m x_G - Y_t) N_v$$

$$D a_{12} = (I_z - N_t) (m - Y_r) - (m x_G - Y_t) (N_r - m x_G),$$

$$D a_{21} = (m - Y_v) N_v - (m x_G - N_v) Y_v,$$

$$D a_{22} = (m - Y_v) (N_r - m x_G) - (m x_G - N_v) (Y_r - m),$$

$$D b_1 = (I_z - N_t) Y_\delta - (m x_G - Y_t) N_\delta,$$

$$Db_2 = (m - Y_v) N_\delta - (mx_G - N\dot{v}) Y_\delta,$$

$$D = (I_z - N_f) (m - Y_v) - (mx_G - Y_f) (mx_G - N\dot{v}).$$

Equations 11 and 12 describe the lateral dynamics of the vehicle for small motions.

## B. FEEDBACK CONTROL

A linear rudder feedback control law based on equations 11 and 12 has the form

$$\delta = k_v v + k_r r, \quad (13)$$

where  $k_v$ ,  $k_r$  are the feedback gains. By substituting equation 13 into 11 and 12 we get the closed loop dynamics equations

$$\dot{v} = (a_{11}u + b_1u^2k_v)v + (a_{12}u + b_1u^2k_r)r, \quad (14)$$

$$\dot{r} = (a_{21}u + b_2u^2k_v)v + (a_{22}u + b_2u^2k_r)r \quad (15)$$

The characteristic equation of 14 and 15 is

$$\lambda^2 + A_1\lambda + A_2 = 0, \quad (16)$$

where

$$A_1 = [a_{11} + a_{22} + (b_1k_v + b_2k_r)u]u,$$

$$A_2 = [a_{11}a_{22} - a_{12}a_{21} + (b_1a_{22} - b_2a_{12})uk_v + (b_2a_{11} - b_1a_{21})uk_r]u^2.$$

Now the desired closed loop characteristic equation is



$$\lambda^2 + \alpha_1 \lambda + \alpha_2 = 0 \quad (17)$$

By equating the coefficients of eqs.16 and 17 we get the following system of linear equations

$$k_v b_1 u^2 + k_r b_2 u^2 = -\alpha_1 - (a_{11} + a_{22}) u, \quad (18)$$

$$k_v (a_{22} b_1 - a_{12} b_2) u^3 + k_r (a_{11} b_2 - a_{21} b_1) u^3 = \alpha_2 - (a_{11} a_{22} - a_{12} a_{21}) u^2 \quad (19)$$

Equations 18 and 19 then determine the gain  $k_v$ ,  $k_r$ , in the feedback control law (Eq.13).

The coefficients  $\alpha_1$ ,  $\alpha_2$  of the desired characteristic equation 17 can be specified according to any standard pole placement design technique. In this work we decide to use the controller time constant,  $T_c$ , as the parameter that specifies the coefficients  $\alpha_1$ ,  $\alpha_2$ . In this way the desired characteristic equation is

$$\left(\lambda + \frac{1}{T_c}\right) = 0 \quad \text{or} \quad \lambda^2 + \frac{2}{T_c} \lambda + \frac{1}{T_c^2} = 0 \quad (20)$$

and comparing with eq.17 we see that

$$\alpha_1 = \frac{2}{T_c}, \quad \alpha_2 = \frac{1}{T_c^2} \quad (21)$$

Specification of a controller time constant  $T_c$  then determines the feedback gains  $k_v$ ,  $k_r$  uniquely.

### C. FEEDFORWARD CONTROL

The control law (Eq.13) guarantees stability of  $v = r = 0$  of equations 11 and 12, in other words straight line motion at an arbitrary heading. When the commanded angular velocity  $r_c$  is nonzero the control law is slightly modified to

$$\delta = k_v v + k_r (r - r_c) + k_c r_c, \quad (22)$$

where  $r_c$  is the commanded turning rate and  $k_c$  is the feedforward gain. This is computed based on steady state accuracy requirements. At steady state, equations 11 and 12 yield

$$v = v_c r_c, \quad \delta = \delta_c r_c \quad (23)$$

where

$$v_c = \frac{b_1 a_{22} - b_2 a_{12}}{b_2 a_{11} - b_1 a_{21}}, \quad \delta_c = \frac{a_{21} a_{12} - a_{11} a_{22}}{b_2 a_{11} - b_1 a_{21}} \quad (24)$$

Substituting equations 23 and 24 into equation 22, and requiring that  $r = r_c$  at steady state, we can solve for  $k_c$ ,

$$k_c = \delta_c - k_v v_c, \quad (25)$$

and the control law (Eq.22) becomes

$$\delta = k_v v + k_r r - (k_r - \delta_c + k_v v_c) r_c. \quad (26)$$

Substituting the values of  $k_r$ ,  $\delta_c$ ,  $k_v$ ,  $v_c$  in (26), we can finally write the control law (Eq.26) in the form

$$\delta = k_v v + k_r r - k_0 a_2 r_c , \quad (27)$$

where

$$k_0 = \frac{1}{(b_2 a_{11} - b_1 a_{21}) u^3} . \quad (28)$$

With the above feed forward gain the control law is complete. It should be mentioned that all gains  $K_v$ ,  $k_r$ ,  $k_0$  depend explicitly on the forward speed  $u$  and are, therefore, continuously updated every time a different forward speed is commanded.

#### D. RESULTS

The response of the control law (Eq.27) applied to the system of Equations 11 and 12 is shown in Figure 2, where the commanded turning rate is 0.1 rad/sec. It can be seen that the actual vehicle turning rate  $r$  converges to its commanded value  $r_c$ , as expected. The gain were computed based on a selected time constant  $T_c = 1$  dimensionless second. Time is nondimensionalized here with respect to the vehicle forward speed  $u = 2$  ft/sec and the vehicle length  $L = 7.3$  ft. Therefore, one dimensionless second corresponds to 3.65 seconds of real time and this is verified by the simulation results of Figure 2 (the response drops about 60% every time constant).

The response for different time constants (in dimensionless seconds) is shown in Figure 3 where it can be

seen that higher values of  $T_c$ , result in slower vehicle response as expected. Similar is the rudder angle response as shown in Figure 4. Smaller values of  $T_c$ , result in tighter control and more rudder activity.

## E. ACCURACY

The feedforward gain  $k_0$  computed from eq.28 ensures that the steady state turning rate  $r$  equals the commanded value  $r_c$  for the linear system of equations 11 and 12. To analyze the effects of nonlinearities we start with the nonlinear equations of motion 3 and 4 and we write them in the form

$$\dot{v} = a_{11}uv + a_{12}ur + b_1u^2\delta + d_v(v, r), \quad (29)$$

$$\dot{r} = a_{12}uv + a_{22}ur + b_2u^2\delta + d_r(v, r), \quad (30)$$

$$Dd_v(v, r) = -0.5QC_D[(I_Z - N_f)I_1 + (Y_f - mx_G)I_2],$$

$$Dd_r(v, r) = -0.5QC_D[(m - Y_v)I_1 + (N_v - mx_G)I_2],$$

$$D = (I_Z - N_f)(m - Y_v) - (mx_G - Y_f)(mx_G - N_v),$$

$$I_1 = \int h(\xi)(v + \xi r)|v + \xi r|d\xi,$$

$$I_2 = \int h(\xi)(v + \xi r)|v + \xi r|\xi d\xi.$$

The values of  $v$  and  $r$  at steady state can then be computed from

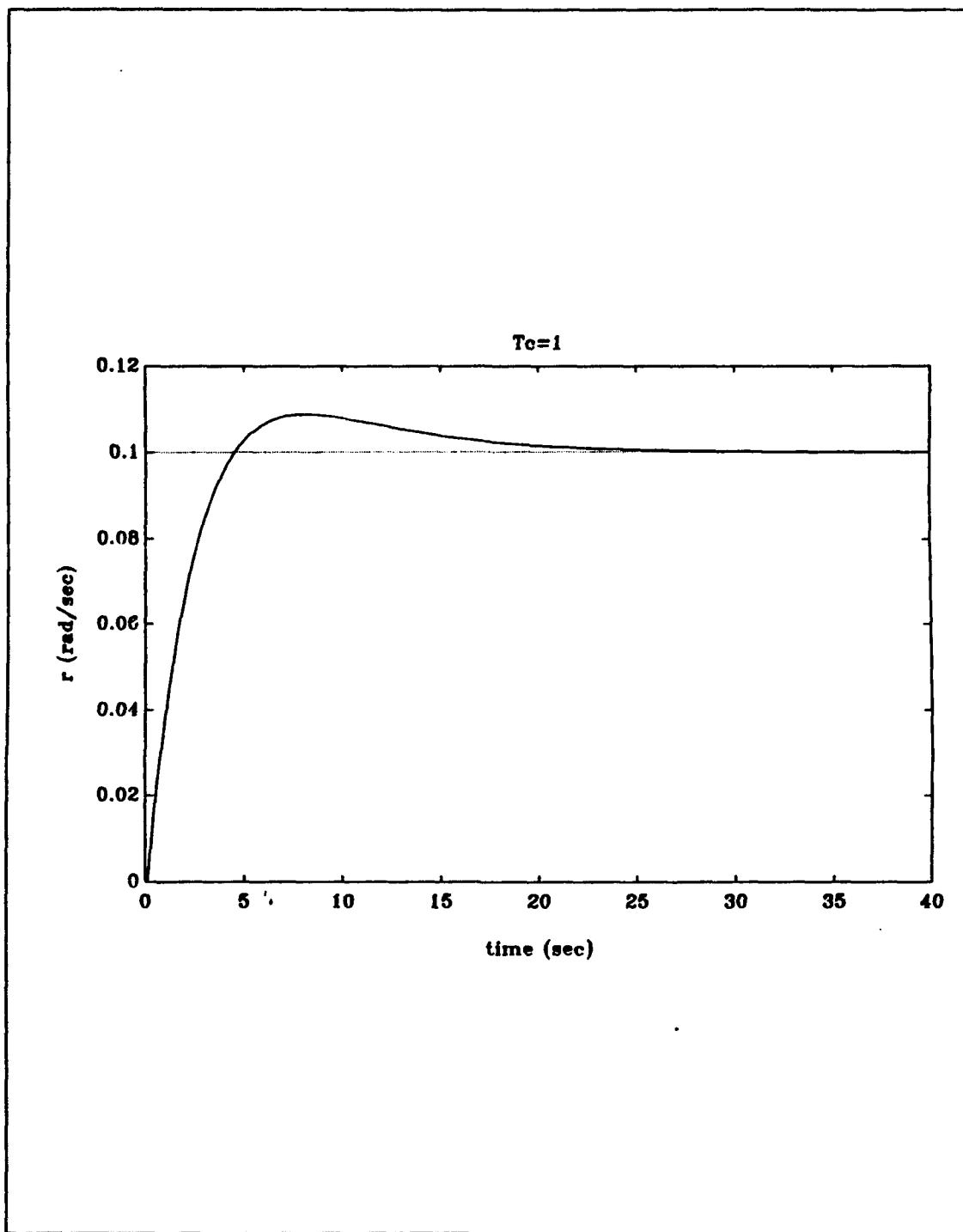


Figure 2. Turning Rate Response for  $T_c=1$ .

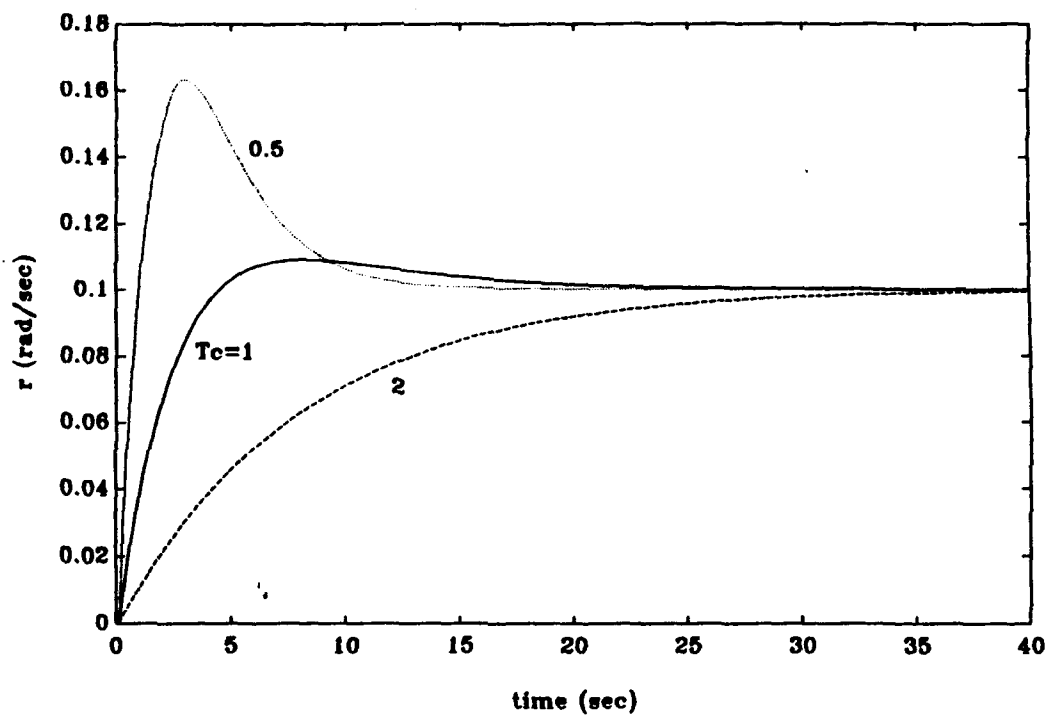


Figure 3. Turning Rate Response for Different Values of  $T_c$ .

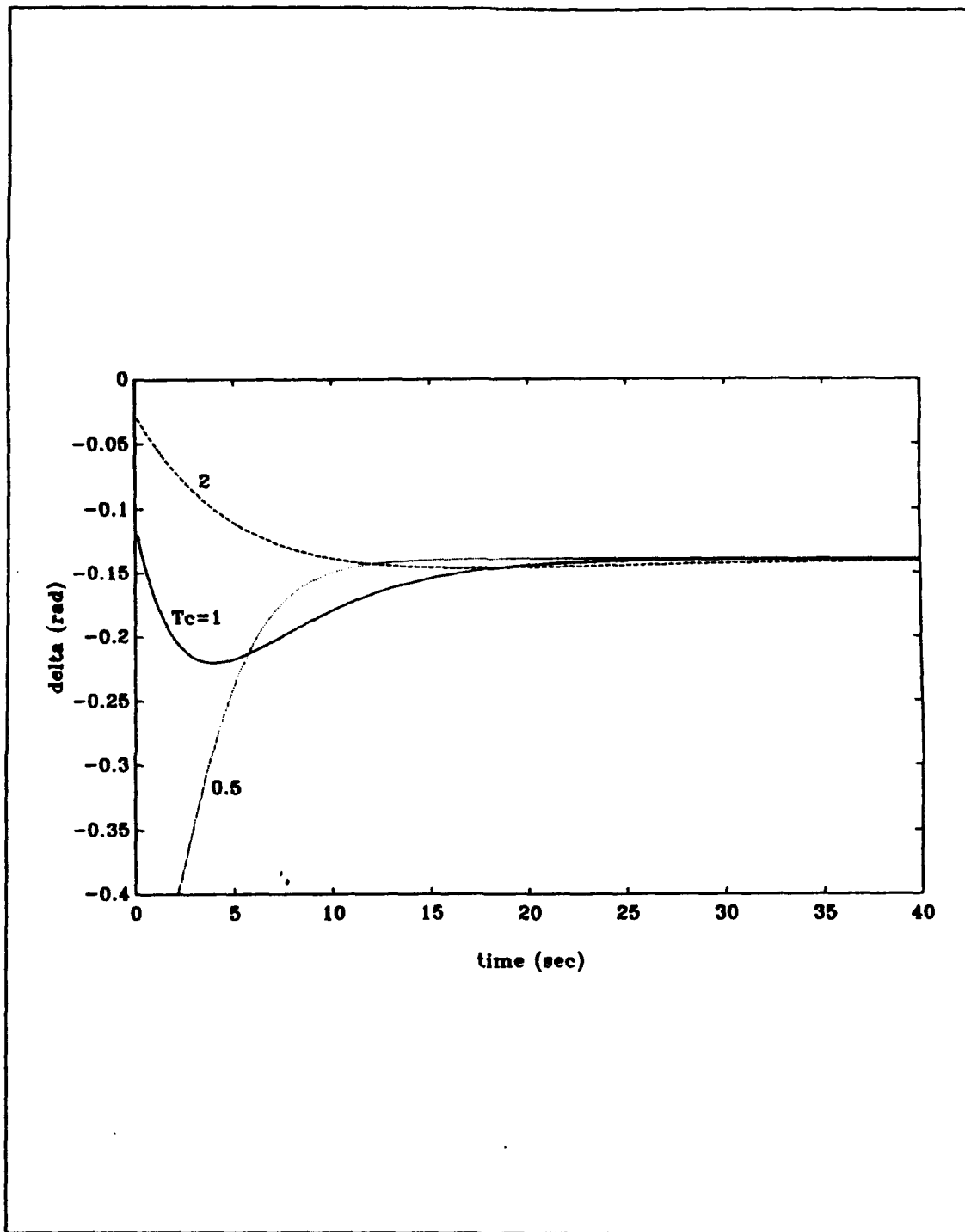


Figure 4. Rudder Angle Time Histories for Different Values of  $T_c$ .

$$a_{11}uv+a_{12}ur+b_1u^2\delta+d_v(v,r)=0 \quad , \quad (31)$$

$$a_{21}uv+a_{22}ur+b_2u^2\delta+d_r(v,r)=0 \quad , \quad (32)$$

$$\delta-k_vv-k_r r+k_0\alpha_2 r_c=0 \quad . \quad (33)$$

The solution to these equations is not  $r = r_c$  unless  $d_r = d_r = 0$ . This is demonstrated by the time simulation of Figure 5, for which the quadratic drag coefficient  $C_D$  was set equal to 0.5. It can be seen that the vehicle turning rate develops a nonzero steady state error with respect to the commanded value of 0.1 rad/sec. As the controller time constant  $T_c$  is decreased, the control law becomes tighter and this steady state error could not become zero due to uncertainties in the vehicle hydrodynamic description and various unmodeled dynamics. Even if  $k_0$  were determined from equations 31 to 33 such that  $r = r_c$ , the uncertainties involved in the determination of the hydrodynamic coefficients in the equations of motion would cause the actual value of  $r$  to be different than the commanded value  $r_c$ . One way to ensure steady state accuracy is to abandon the use of the feedforward gain  $k_0$  and to introduce integral control. This possibility is examined in the next section.



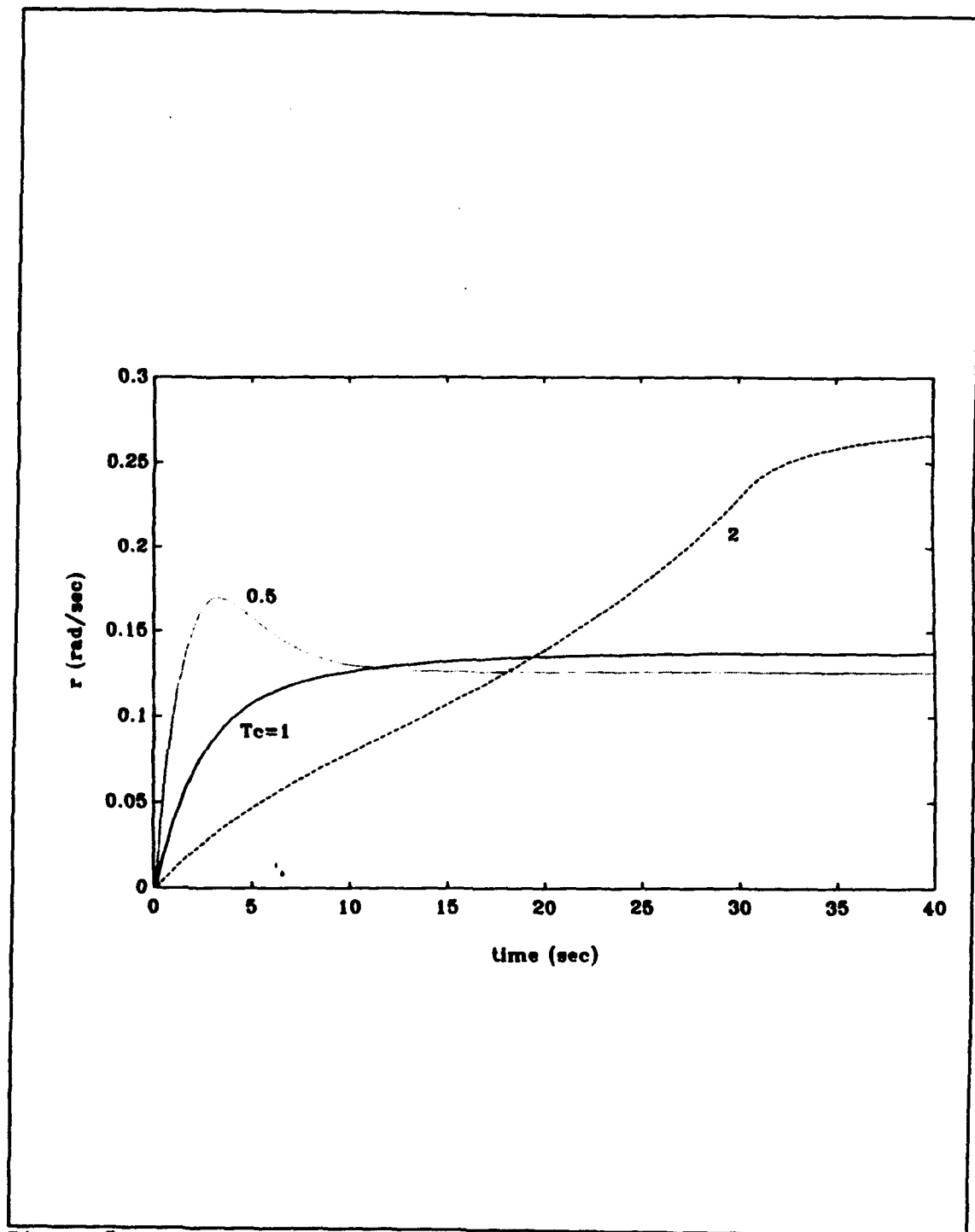


**Figure 5.** Turning Rate Response for Different Values of  $T_c$  and for Nonzero Drag Coefficient.

## F. INTEGRAL CONTROL

An alternative way to ensure stability and convergence to the commanded value  $r_c$  is to introduce integral control in the form

$$\delta = k_v v + k_r (r - r_c) + k_I \int (r - r_c) dt \quad (34)$$

In that case, the system of state equations is augmented by the additional

$$\dot{r}_I = r - r_c \quad (35)$$

In order to compute the gains  $k_v$ ,  $k_r$ ,  $k_I$  we set  $r_c = 0$  and substitute the control law

$$\delta = k_v v + k_r r + k_I r_I, \quad (36)$$

into equations 11 and 12. The resulting closed loop system is

$$\dot{v} = (a_{11}u + k_v b_1 u^2) v + (a_{12}u + k_r b_1 u^2) r + k_I b_1 u^2 r_I \quad (37)$$

$$\dot{r} = (a_{21}u + k_v b_2 u^2) v + (a_{22}u + k_r b_2 u^2) r + k_I b_2 u^2 r_I \quad (38)$$

$$\dot{r}_I = r \quad (39)$$

The characteristic equation of equations 37 to 39 can be computed as

$$\lambda^3 + A_1 \lambda^2 + a_2 \lambda + a_3 = 0 \quad (40)$$

where

$$A_1 = -(a_{11} + a_{22})u - b_1 u^2 k_v - b_2 u^2 k_r ,$$

$$A_2 = (a_{11}a_{22} - a_{21}a_{12})u^2 + (a_{11}b_2 - a_{21}b_1)u^3 k_r + \\ + (a_{22}b_1 - a_{12}b_2)u^3 k_v - b_2 u^2 k_r ,$$

$$A_3 = (a_{11}b_2 - a_{21}b_1)u^3 k_r .$$

If the desired characteristic equation is

$$\lambda^3 + \alpha_1 \lambda^2 + \alpha_2 \lambda + \alpha_3 = 0 \quad (41)$$

by equating the coefficients of equations 40 and 41 we get the following system of linear equations which determines the three gains  $k_v$ ,  $k_r$ ,  $k_I$ :

$$k_v b_1 u^2 + k_r b_2 u^2 = -\alpha_1 - (a_{11} + a_{22})u ,$$

$$k_v (a_{22}b_1 - a_{12}b_2)u^3 + k_r (a_{11}b_2 - a_{21}b_1)u^3 = \alpha_2 + k_r b_2 u^2 \\ - (a_{11}a_{22} - a_{21}a_{12})u^2 ,$$

$$k_r (a_{11}b_2 - a_{21}b_1)u^3 = \alpha_3 .$$

For a time constant  $T_c$  and an integrator time constant  $T_I$ , the desired characteristic equation becomes

$$\left(\lambda + \frac{1}{T_c}\right)^2 \left(\lambda + \frac{1}{T_I}\right) = 0 ,$$

or

$$\lambda^3 + \left(\frac{1}{T_I} + \frac{2}{T_c}\right)\lambda^2 + \left(\frac{1}{T_c^2} + \frac{2}{T_I T_c}\right)\lambda + \frac{1}{T_c^2 T_I} = 0 ,$$

so that

$$\alpha_1 = \frac{1}{T_I} + \frac{2}{T_c} ,$$

$$\alpha_2 = \frac{1}{T_c^2} + \frac{2}{T_I T_c} ,$$

$$\alpha_3 = \frac{1}{T_c^2 T_I} .$$

With these choices the determination of the gain  $k_v$ ,  $k_r$ ,  $k_I$ , is complete. A numerical simulation for  $r_o = 0.1$  rad/sec. and with  $C_p = 0.5$  is presented in Figure 6. The time constants are  $T_o = 1$  and  $T_I$ , assumed the three different values shown in the figure. It can be seen that despite the nonlinear drag terms, steady state accuracy is achieved. Since the response of systems compensated by integral control action tends to be more oscillatory, in this work we will use the previous feedforward control. As we show in the next chapter, steady state accuracy is guaranteed once the control law is combined with a suitable guidance.

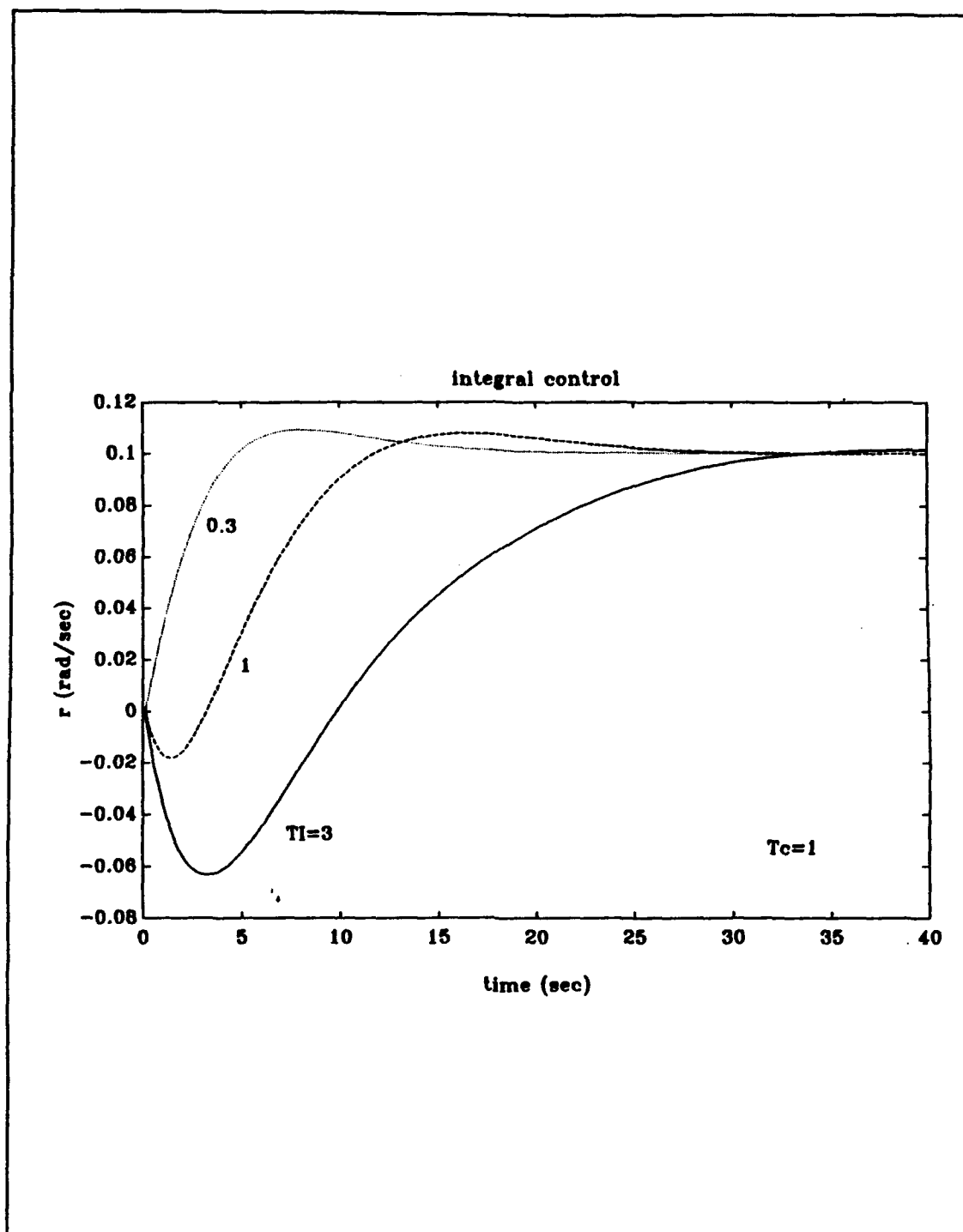


**Figure 6.** Turning Rate Response for  $T_c=1$ , Different Values of  $T_I$ , Nonzero Drag Coefficient, and Use of Integral Control.

#### IV. GUIDANCE LAW

##### A. GENERAL

The previously developed control law is able to deliver a vehicle commanded turning rate  $r_c$ . In order to achieve path control to a commanded route in the horizontal plane, however, the commanded turning rate  $r_c$  must be appropriately selected. This constitutes the guidance law design. Two such guidance laws are described in the following, cross track error and proportional guidance. Without loss of generality, we assume that the commanded path is a straight line. This is not a very restrictive assumption since every smooth path can be discretized into a series of straight line segments as accurately as desired.

##### B. CROSS TRACK ERROR GUIDANCE

The guidance law is based solely on kinematics, whereas vehicle dynamics are handled by the control law. Guidance law development based on

$$\dot{\psi} = r_c \quad (42)$$

$$\dot{y} = u \sin \psi, \quad (43)$$

where  $r_c$  is the commanded turning rate and the lateral velocity  $v$  is assumed to be zero in equation 43.

Cross track error guidance is achieved by

$$r_c = k_\psi \psi + k_y y \quad (44)$$

By substituting equation 44 into equation 42 we get the closed loop guidance system

$$\dot{\psi} = k_\psi \psi + k_y \dot{y} , \quad (45)$$

$$\dot{y} = u \sin \psi , \quad (46)$$

The characteristic equation of equations 45 and 46 is obtained by making the small angle approximation  $\sin \psi = \psi$ , and is

$$\lambda^2 - k_\psi \lambda - k_y u = 0 . \quad (47)$$

If the desired characteristic equation is

$$\lambda^2 + \beta_1 \lambda + \beta_2 = 0 , \quad (48)$$

the guidance law gains  $k_\psi$ ,  $k_y$  are obtained by equating the coefficients of equations 47 and 48

$$k_\psi = -\beta_1 , \quad (49)$$

$$k_y = -\frac{\beta_2}{u} . \quad (50)$$

Analogously to the control law design, if the time control of the guidance law is selected to be  $T_G$ , then equations 49 and 50 result in

$$k_\psi = -\frac{2}{T_G} , \quad (51)$$

$$k_y = -\frac{1}{T_G^2 u} . \quad (52)$$

Selection of  $T_0$  then determines  $k_\psi$ ,  $k_y$  directly.

Although this development followed the small angle approximation, it is not difficult to see that negative values of  $k_\psi$  and  $k_y$  will guarantee stability of the nonlinear system of equations 45 and 46. The associated total energy of the system is

$$E(\dot{\psi}, \psi) = \frac{1}{2} \dot{\psi}^2 - k_y u (1 - \cos \psi) , \quad (53)$$

which can be viewed as the sum of kinetic and potential energy. Using equation 45, this is written as

$$E(\psi, y) = \frac{1}{2} (k_\psi \psi + k_y y)^2 - k_y u (1 - \cos \psi) . \quad (54)$$

We note that  $E(\psi, y)$  provides a Liapunov function for equations 45 and 46, since  $E(0,0)=0$  at the unique equilibrium  $(\psi, y)=(0,0)$  and  $E(\psi, y)>0$  for  $(\psi, y) \neq (0,0)$ , because  $k_y < 0$ . Moreover, we have

$$\dot{E} = \frac{dE}{d\psi} \times \frac{d\psi}{dt} + \frac{dE}{dy} \times \frac{dy}{dt} = \frac{dE}{d\psi} \dot{\psi} + \frac{dE}{dy} \dot{y} . \quad (55)$$

Evaluating the indicated partial derivatives we get

$$\frac{dE}{d\psi} = (k_\psi \psi + k_y y) k_\psi - k_y u \sin \psi , \quad (56)$$

$$\frac{dE}{dy} = (k_\psi \psi + k_y y) k_y . \quad (57)$$



Substituting equations 45, 46, 56 and 57 into equation 55 we find

$$\dot{E} = k_{\psi}(k_{\psi}\psi + k_y y)^2, \quad (58)$$

which is negative. Therefore, Liapunov's theorem guarantees asymptotic stability of the nonlinear system (equations 45 and 46).

### C. PROPORTIONAL GUIDANCE

A typical orientation based guidance law is pursuit guidance which is accomplished as follows: The commanded vehicle heading angle  $\psi_c$  equals the line of sight angle between the vehicle and a target point D located ahead of the vehicle and a constant preview distance  $d$  on the nominal straight line path as shown in Figure 1. In other words

$$\psi_c = -\tan^{-1} \frac{Y}{d}. \quad (59)$$

In a proportional guidance scheme a time constant  $T$  is incorporated in the above line of sight equation

$$T\dot{\psi}_c + \psi_c = -\tan^{-1} \frac{Y}{d}, \quad (60)$$

and we arrive at the proportional guidance which is used here for path control

$$T\dot{r}_c + \psi = -\tan^{-1} \frac{Y}{d}, \quad (61)$$

$$r_c = -\frac{1}{T}\psi - \frac{1}{T}\tan^{-1}\frac{y}{d} . \quad (62)$$

The linearized form of equation 62 is

$$r_c = -\frac{1}{T}\psi - \frac{1}{Td}y , \quad (63)$$

and by comparing it to equations 48 through 50 we can see that it corresponds to a guidance characteristic equation with

$$\beta_1 = \frac{1}{T} , \quad (64)$$

$$\beta_2 = \frac{u}{Td} . \quad (65)$$

## V. STABILITY

### A. SIMULATIONS

In order to assess stability of the combined guidance and control law we proceed first by a series of numerical integrations. The simulations are based on the dynamical equations 3 and 4 and the kinematic equations 6 and 8. The rudder control law in the form of equation 27 is used, while the cross track error guidance (eq.44) is employed. Results are presented in terms of the lateral deviation  $y$  in ft versus time  $t$  in seconds. Figure 7 shows the vehicle response for control time constant  $T_c=0.5$  and guidance time constant  $T_g=1$ . It can be seen that the response is stable, although it exhibits slow convergence characteristics to the commanded path  $y=0$ . To speed-up speed of response we could lower the guidance time constant  $T_g$ . The results of the simulation for  $T_c=0.5$  and  $T_g=0.5$  are presented in Figure 8. It can be seen that the convergence is now faster although the path overshoot is higher. If we maintain the same guidance time constant  $T_g=0.5$  and increase the control time constant  $T_c=2$ , the vehicle is unstable as demonstrated by Figure 9. The response exhibits now oscillatory characteristics or a limit cycle. The explanation for this phenomenon is that, in this case the control law is very slow and the rudder cannot follow the

commanded turning rates by the guidance law which is considerably faster, due to its smaller time constant. To remedy this instability we should either lower  $T_c$  as in Figure 8 demonstrated, or increase the value of  $T_c$ . The results of this simulation are shown in Figure 10, for which  $T_c=2$  and  $T_c=2$ . The response exhibits now characteristics of a damped oscillation and is stable, although convergence is very slow and oscillatory.

## B. STABILITY

The previous simulation results show that there exists a certain range of  $(T_c, T_g)$  combinations that results in stable response. In order to compute this range and verify the numerical integration results, we use the linearized equations of motion

$$\dot{\psi} = r \quad (66)$$

$$\dot{v} = a_{11}uv + a_{12}ur + b_1u^2\delta, \quad (67)$$

$$\dot{r} = a_{21}uv + a_{22}ur + b_2u^2\delta, \quad (68)$$

$$\dot{y} = u\psi + v \quad (69)$$

the rudder control law

$$\delta = k_v v + k_r r - k_o \alpha_2 r_c, \quad (70)$$

and the turning rate guidance law

$$r_c = k_\psi \psi + k_y y. \quad (71)$$

In a compact vector notation the linearized equations of motion 66 through 71 are written as

$$\dot{\chi} = A\chi, \quad \chi = [\psi, v, r, y] \quad (72)$$

Motion stability is established by the eigenvalues of matrix A, if all eigenvalues have negative real parts the nominal straight line motion is dynamically stable, while if at least one eigenvalue of A is positive, the system is unstable. Writing out the characteristic equation of equation 72 we get

$$\lambda^4 + B\lambda^3 + C\lambda^2 + D\lambda + E = 0, \quad (73)$$

where

$$B = \alpha_1, \quad (74)$$

$$C = \alpha_2 - (b_1\beta_2 + b_2u\beta_1)uk_o\alpha_2, \quad (75)$$

$$D = \alpha_2\beta_1 + d_1\alpha_2\beta_2, \quad (76)$$

$$E = \alpha_2\beta_2, \quad (77)$$

and

$$d_1 = -\frac{b_2 + b_2a_{12} - b_1a_{22}}{(b_2a_{11} - b_1a_{21})u}, \quad (78)$$

In the derivation of expressions 74 to 78 we have used equations 18 and 19 for the feedback gains, equation 28 for the feedforward gain, and equations 49 and 50 for the general guidance law gains.

If we apply Routh's criterion to the fourth order equation 73 we can find the following critical condition for stability

$$BCD - B^2E - D^2 > 0 . \quad (79)$$

If we substitute equations 74 through 77 in equation 79, we find the following condition

$$\alpha_1 \alpha_2 \left[ 1 - \left( \frac{b_1}{u} \beta_2 + b_2 \beta_1 \right) u^2 k_o \right] (\beta_1 + d_1 \beta_2) - \alpha_1^2 \beta_2 - \alpha_2 (\beta_1 + d_1 \beta_2)^2 = 0 \quad (80)$$

Equation 80 represents in algebraic form the critical condition for stability in terms of the control law characteristic equation coefficients  $\alpha_1$ ,  $\alpha_2$  and the guidance law coefficients  $\beta_1$ ,  $\beta_2$ . It can be used for both the cross track error and the proportional guidance schemes, if we employ the appropriate expressions for  $\beta_1$ ,  $\beta_2$  from Chapter IV.

For the case of cross track error guidance, equation 80 results in

$$T_c = \frac{2 [T_G^2 - (b_1 + 2b_2 T_G u) u k_o] (2T_G + d_1)}{4T_G^2 + (2T_G + d_1)^2} \quad (81)$$

For a given guidance law time constant  $T_G$ , equation 81 specifies the critical control time constant for stability.

Stability of the combined guidance and control scheme is guaranteed for values of  $T_c$  that are less than the critical value computed from equation 81. For  $T_c$  values above the critical value (eq.80) the system is unstable. In these cases, one pair of complex conjugate eigenvalues of matrix A

in equation 72 has positive real parts, and as a result the response of the system is oscillatory.

A plot of the critical stability condition (Eq.81) is shown in Figure 11. the response is stable for  $(T_a, T_o)$  combinations that lie below the critical curve. The number 1 through 4 on the figure correspond to the four numerical simulations that were presented in Figure 7 through 10, respectively. It can be seen that the simulation results agree with the stability analysis performed in this section. Point 3 is located above the critical curve and the results in the unstable oscillatory response observed in Figure 9.

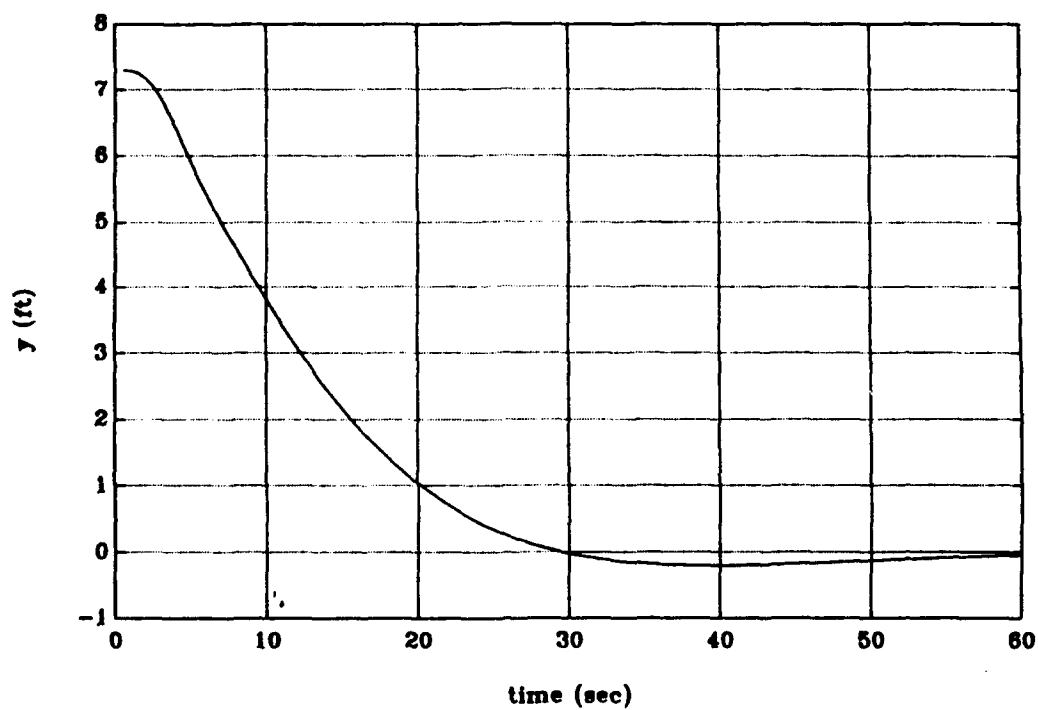


Figure 7. Path Keeping Response for  $T_c=0.5$ ,  $T_e=1$ .



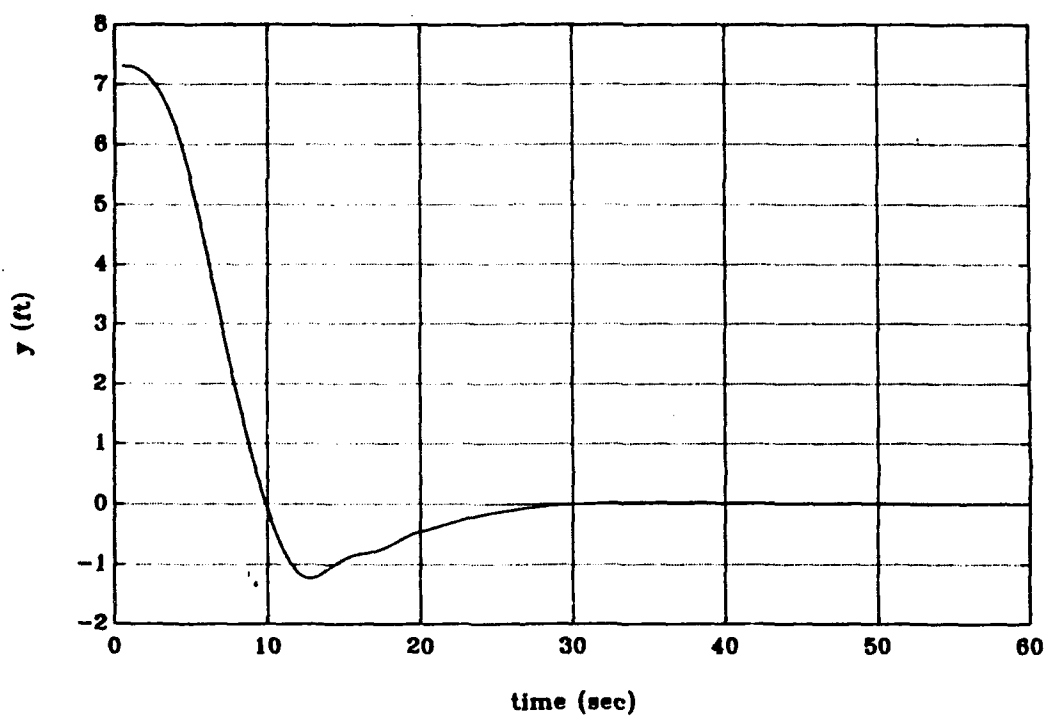


Figure 8. Path Keeping Response for  $T_c=0.5$ ,  $T_o=0.5$ .

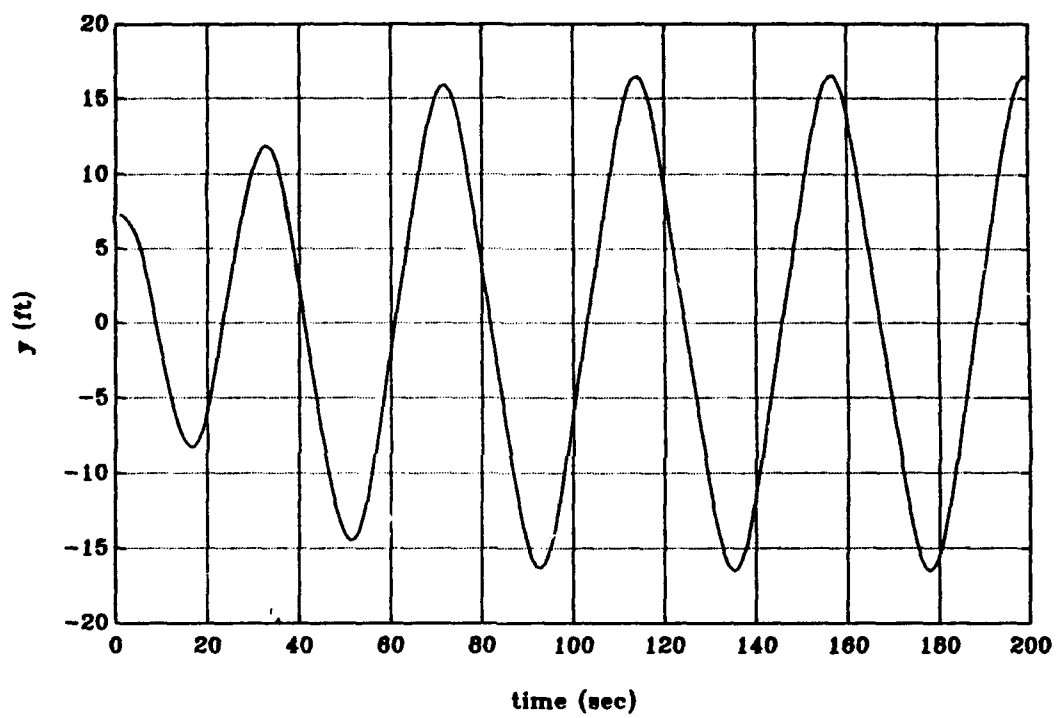


Figure 9. Path Keeping Response for  $T_c=2$ ,  $T_o=0.5$ .

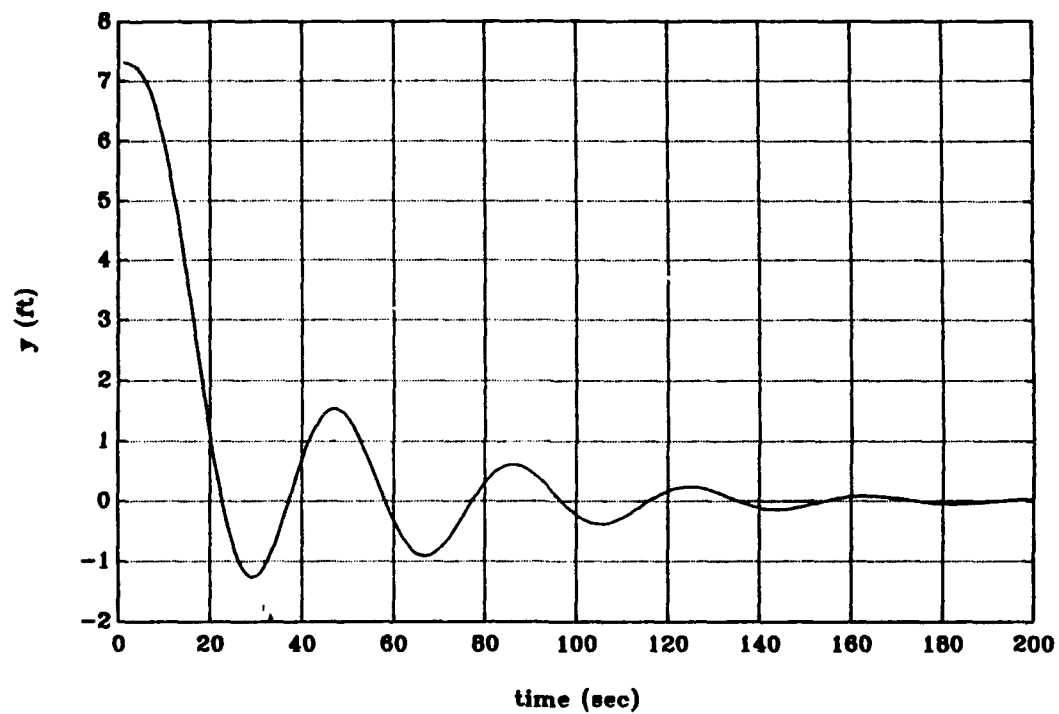


Figure 10. Path Keeping Response for  $T_c=2$ ,  $T_o=2$ .

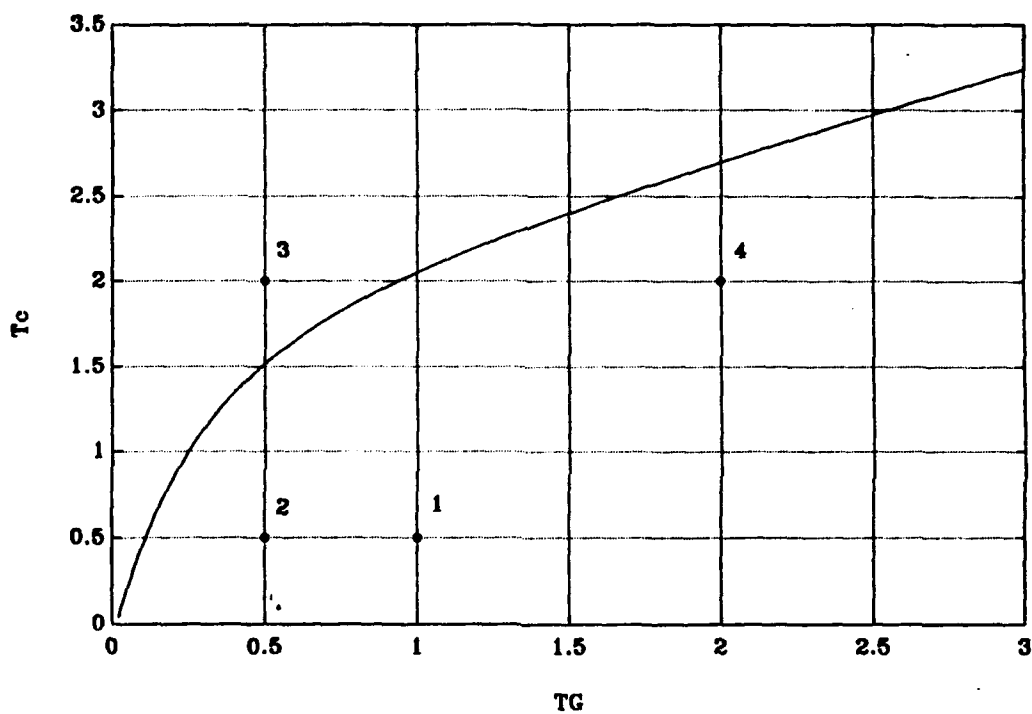


Figure 11. Critical  $T_c$ ,  $T_G$  Curve for Stability.

## VI. CONCLUSIONS AND RECOMMENDATIONS

The goal of this work, stability analysis of turning rate guidance and control for autonomous vehicles has been achieved. The control law was based on the dynamic equations in sway and yaw. The feedback gains were analytically computed by pole-placement techniques and the feedforward gain was evaluated based on the desired steady-state accuracy.

The guidance laws that were utilized, cross-track error or proportional guidance, were based on the kinematics relations. It was found that unless the guidance and control laws were designed according to certain conditions, stability of the system was not guaranteed. These stability conditions were computed analytically and the results were verified by numerical simulations. Recommendations for future work include an analysis of the performance of turning-rate guidance and control from the point of view of sensitivity to sensor noise, state estimation, and disturbance rejection. Comparisons with other guidance and control laws, such as line of-sight guidance, should also be performed.

## LIST OF REFERENCES

1. Healey, A.J., McGhee, R.B., Cristi, R., Papoulias, F.A., Kwak, S.H., Kanayama, Y., and Lee, Y. [1990] "Mission planning, execution, and data analysis for the NPS AVU II autonomus underwater vehicle", Proceedings, NSF Workshop on Mobile Undersea Robotics, Monterey, CA.
2. Papoulias, F.A. [1991] "Bifurcation analysis of line of sight vehicle guidance using sliding modes", International Journal of Bifurcation and Chaos, 1, 4.
3. Friedland, B. [1986] *Control System Design: An Introduction to State-Space Methods* (McGraw-Hill, New York).
4. Kanayama, Y., Kimura, Y., Noguchi, T., and Miyazaki, F. [1990] "A stabletracking control method for an autonomus mobile robot", Proceedings, IEEE International Conference on Robotics and Automation, Cincinnati, Ohio.
5. Bahrke, F. [1992] "On-line identification of the speed, steering and diving response parameters of an autonomus underwater vehicle from experimental data", Mechanical Engineer's Thesis, Naval Postgraduate School, Monterey, California.

# INITIAL DISTRIBUTION LIST

1. Defense Technical Information Center 2  
Cameron Station  
Alexandria, VA 22304-6145
2. Library, Code 052 2  
Naval Postgraduate School  
Monterey, CA 93943-5002
3. Chairman, Code AA 1  
Department of Aeronautics  
and Astronautics  
Naval Postgraduate School  
Monterey, CA 93943
4. Professor L. V. Schmidt 1  
Code AA/SC  
Naval Postgraduate School  
Monterey, CA 93943
5. Professor F. A. Papoulas 1  
Code ME/Pa  
Naval Postgraduate School  
Monterey, CA 93943

- |    |                                |   |
|----|--------------------------------|---|
| 6. | Hellenic Army General Staff    | 3 |
|    | Technical Directorate          |   |
|    | Stratopedon Papagou, Cholargos |   |
|    | Athens, Greece                 |   |
| 7. | Embassy of Greece              | 1 |
|    | Defence and Army Attache       |   |
|    | 2228 Massachusetts Ave., N. W. |   |
|    | Washington, D. C. 20008        |   |
| 8. | Ioannis Kapelios               | 1 |
|    | Philippou Ioannou 21,          |   |
|    | Volos, GREECE                  |   |